Abnormal Functional Connectivity in Radiologically Isolated Syndrome: A Resting-State fMRI Study

Journal:	*Multiple Sclerosis Journal*
Manuscript ID	MSJ-23-0039.R3
Manuscript Type:	Original Research Paper
Date Submitted by the Author:	30-Jul-2023
Complete List of Authors:	Benito-Leon, Julian; 12th of October University Hospital, Neurology del Pino, Ana Belén; URJC, Medical Image Analysis Laboratory Aladro, Yolanda; Getafe University Hospital, Department of Neurology Cuevas, Constanza; 12th of October University Hospital, Neurology Santos, Ángela; Hospital Universitario 12 de Octubre, Department of Neurology Galan Sánchez-Seco, Victoria; 12th of October University Hospital, Neurology Labiano-Fontcuberta, Andrés; 12th of October University Hospital, Neurology Gómez López, Ana; Hospital Universitario 12 de Octubre, NEUROLOGY Salgado-Cámara, Paula; Hospital Universitario 12 de Octubre, Neurology Costa-Frossard França, Lucienne; Hospital Universitario Ramon y Cajal, Neurology Department Monreal, Enric; Hospital Universitario Ramon y Cajal, Neurology Sainz de la Maza , Susana ; Hospital Universitario Ramon y Cajal, Neurology Department Matias-Guiu, Jordi A.; Hospital Clinico Universitario San Carlos, Neurology Matias-Guiu, Jorge; Hospital Clinico Universitario San Carlos, Neurology Delgado-Alvarez, Alfonso; Hospital Clinico Universitario San Carlos, Neurology Montero, Paloma; Hospital Clinico Universitario San Carlos, Neurology Martínez-Ginés, Maria Luisa; Hospital General Universitario Gregorio Marañón, Neurology Higueras, Yolanda; Hospital General Universitario Gregorio Marañón, Neurology Ayuso-Peralta, Lucía; Hospital Universitario Príncipe de Asturias, Neurology Malpica, Norberto; URJC, Medical Image Analysis Laboratory

	Melero, Helena; Complutense University of Madrid, Psychobiology and Methodology of Behavioural Sciences
Keywords:	MRI, Functional MRI, Radiologically Isolated Syndrome
Abstract:	Background: Radiologically isolated syndrome (RIS) patients might have psychiatric and cognitive deficits, which suggests an involvement of executive attention neuronal networks. Notwithstanding, very little is known about the neural networks involved in RIS, and further study is needed. Objective: To examine functional connectivity differences between RIS and healthy controls (HCs) using resting-state functional MRI (fMRI). Methods: Resting-state fMRI data in 25 RIS patients and 28 HCs were analyzed using independent component analysis and seed-based correlation analysis. Participants also underwent neuropsychological testing. Results: RIS patients and HCs did not differ in age, sex, and education. However, RIS patients' cognitive performance was significantly worse in verbal and visuospatial learning, memory, attention, information processing speed, semantic verbal fluency, and executive functions. Relative to HCs, RIS patients showed higher connectivity in resting-state neural networks involved in cognitive processes (default mode and central executive networks). Furthermore, the seed-based correlation analysis revealed higher functional connectivity in RIS patients of the posterior cingulate cortex, a hub of functional neural networks. Conclusions: RIS patients had abnormal brain connectivity in major resting-state neural networks that might be involved in cognitive features. This entity should be considered not an "incidental finding" but an exclusively nonmotor (neurocognitive) variant of multiple sclerosis.

Abnormal Functional Connectivity in Radiologically Isolated Syndrome: A Resting-State fMRI Study

Julián Benito-León, M.D., Ph.D;[1,2,3] † Ana Belén del Pino;[4] † Yolanda Aladro, M.D., Ph.D.;[5,6] Constanza Cuevas, M.A. Psych.;[1] Ángela Domingo-Santos, M.D, Ph.D.;[1] Victoria Galán Sánchez-Seco, M.D., Ph.D.;[1] Andrés Labiano-Fontcuberta, M.D.;[1] Ana Gómez-López, M.D.;[1] Paula Salgado-Cámara, M.D., Ph.D.;[1] Lucienne Costa-Frossard, M.D.;[7] Enrique Monreal, M.D.;[7] Susana Sainz de la Maza, M.D.;[7] Jordi A. Matias-Guiu, M.D., Ph.D.;[8] Jorge Matias-Guiu, M.D., Ph.D.;[8] Alfonso Delgado-Álvarez, M.A. Psych.;[8] Paloma Montero-Escribano, M.D.;[8] Mª Luisa Martínez-Ginés, M.D., Ph.D.;[9] Yolanda Higueras, M.A. Psych.;[9] Lucía Ayuso-Peralta, M.D., Ph.D.;[10] Norberto Malpica, Ph.D.;[4] ‡ Helena Melero, Ph.D.[11] ‡

† These authors contributed equally to this work and should be considered joint first authors

‡ These authors contributed equally to this work and should be considered joint senior authors.

Department of Neurology,[1] University Hospital "12 de Octubre", Madrid, Spain; Centro de Investigación Biomédica en Red Sobre Enfermedades Neurodegenerativas (CIBERNED),[2] Madrid, Spain; Department of Medicine,[3] Faculty of Medicine, Complutense University, Madrid, Spain; Medical Image Analysis Laboratory (LAIMBIO),[4] Rey Juan Carlos University, Móstoles, Madrid, Spain; Department of Neurology,[5] University Hospital of Getafe, Madrid, Spain; Faculty of Biomedical and Health Sciences,[6] European University of Madrid,

Madrid, Spain. Department of Neurology[7] University Hospital "Ramón y Cajal", Madrid, Spain; Department of Neurology,[8] Hospital Clínico "San Carlos" and Instituto de Investigación Sanitaria San Carlos (IdISSC), Madrid, Spain; Department of Neurology,[9] University Hospital "Gregorio Marañón", Madrid, Spain; Department of Neurology,[10] University Hospital "Príncipe de Asturias", Alcalá de Henares (Madrid), Spain; Departamento de Psicobiología y Metodología en Ciencias del Comportamiento,[11] Universidad Complutense, Madrid, Spain

Corresponding author: Dr. Julián Benito-León (jbenitol67@gmail.com)

Running title: Resting-State fMRI in Radiologically Isolated Syndrome

Word count: Abstract: 200; **Text:** 3,991; **References:** 49; **Tables:** 3; **Figures:** 2.

Keywords: Magnetic resonance imaging; Radiologically Isolated Syndrome; Resting-State fMRI.

Acknowledgments.

We want to thank Miss Cristina Martín-Arriscado for her help in the statistical analyses. J. Benito-León is supported by the National Institutes of Health, Bethesda, MD, USA (NINDS #R01 NS39422), the European Commission (grant ICT-2011-287739, NeuroTREMOR), the Ministry of Economy and Competitiveness (grant RTC-2015-3967-1, NetMD—platform for the tracking of

movement disorder), and the Spanish Health Research Agency (grant FIS PI12/01602 and grant FIS PI16/00451).

Abnormal Functional Connectivity in Radiologically Isolated Syndrome: A Resting-State fMRI Study

Abstract. Background: Radiologically isolated syndrome (RIS) patients might have psychiatric and cognitive deficits, which suggests an involvement of major resting-state functional networks. Notwithstanding, very little is known about the neural networks involved in RIS. **Objective:** To examine functional connectivity differences between RIS and healthy controls using resting-state functional MRI (fMRI). **Methods:** Resting-state fMRI data in 25 RIS patients and 28 healthy controls were analyzed using an independent component analysis; additionally, seed-based correlation analysis was used to obtain more information about specific differences in the functional connectivity of resting-state networks. Participants also underwent neuropsychological testing. **Results:** RIS patients did not differ from the healthy controls regarding age, sex, and years of education. However, in memory (verbal and visuospatial) and executive functions, RIS patients' cognitive performance was significantly worse than the healthy controls. In addition, fluid intelligence was also affected. Sixteen out of 25 (64%) RIS patients failed at least one cognitive test, and nine (36.0%) had cognitive impairment. Compared to healthy controls, RIS patients showed higher functional connectivity between the default mode network and the middle and superior frontal gyri; and between the central executive network and the thalamus ($p_{FDR}<0.05$; corrected). In addition, the seed-based correlation analysis revealed that RIS patients presented higher functional connectivity between the posterior cingulate cortex, an important hub in neural networks,

and the precuneus. **Conclusions**: RIS patients had abnormal brain connectivity in major resting-state neural networks and worse performance in neurocognitive tests. This entity should be considered not an "incidental finding" but an exclusively non-motor (neurocognitive) variant of multiple sclerosis.

Keywords: Radiologically isolated syndrome; Multiple sclerosis; Functional connectivity; Resting-state neural networks.

INTRODUCTION

The term "radiologically isolated syndrome" (RIS), coined in 2009 by Okuda et al. [1], refers to the incidental brain magnetic resonance imaging (MRI) finding of white matter lesions suggestive of multiple sclerosis (MS) with evidence of spatial dissemination in subjects with normal neurologic examination and no history of typical MS symptoms.

Given its rarity, it is unsurprising that, compared to MS, only some articles have addressed this entity's basic scientific issues using advanced neuroimaging techniques.[2]–[5] Although RIS cannot be still included in the MS spectrum,[6] more than half of RIS patients experience their first clinical event within ten years of the index MRI, indicating that it is much more than a radiological finding.[7]

RIS brain damage beyond apparent T2 white matter lesions remains mainly unknown. A study demonstrated that RIS patients had significantly lower normalized cortical, thalamic volumes and thinning in several cortical areas, primarily distributed in the frontal and temporal lobes, than healthy controls.[3] Of interest is that thalamic involvement has been observed in another study.[8] The thalamus is acknowledged as a passive triage center and a contributor to cognitive functions like attention, processing speed, and memory because of its intrinsic function as a relay and integration center and participation in several thalamocortical networks.[9]

Cognition is a critical domain of MS research, and understanding the cognitive dysfunction in RIS patients might contribute to the overall understanding of these demyelinating processes. Cognitive deficits in RIS have been associated with a higher likelihood of progressing to clinically definite MS,

even without clinical symptoms.[5] Hence, studying cognitive function in RIS might help clinicians determine the need for closer follow-up and potential disease-modifying interventions. It is known that RIS patients might have non-motor symptoms such as psychiatric (e.g., depression)[10] and cognitive deficits in specific aspects of neuropsychological function, particularly in processing speed and executive functions,[5],[11]–[13] which suggests alterations of the executive attention neuronal networks. Nonetheless, very little is known about the underlying causes of the modifications in the neural networks of RIS patients and their involvement in non-motor manifestations; hence, further study is needed.

Resting-state functional magnetic resonance imaging (fMRI) is an advanced neuroimaging technique to investigate functional connectivity in the brain.[14]–[16] This approach can uncover complex functional networks and provide insights into brain organization that may not be apparent with task-specific fMRI.[14]–[16] Changes in neural networks have been identified in several neurological and psychiatric diseases without obvious structural modifications, indicating the method's high sensitivity.[14]–[16] Also, resting-state fMRI data analysis often involves data-driven approaches like independent component or seed-based correlation analyses.[14]–[16] These methods allow for an exploratory examination of functional connectivity patterns without relying on a priori knowledge or assumptions about task-related activations.[14]–[16] Only one resting-state functional connectivity study has been conducted in RIS patients, and no differences were found compared to healthy controls.[17]

The aim of conducting a new resting-state fMRI study in RIS is to gain insights into the functional alterations occurring in the brain at this early stage and identify early biomarkers or predictive factors for the subsequent development of clinical MS. In the current study, resting-state fMRI data were analyzed using an independent component; specifically, we assessed the following resting-state neural networks: default mode network (DMN), central executive network, frontoparietal networks (left- and right-lateralized), sensorimotor, cerebellar, auditory/language, and visual networks. Additionally, following the procedures used to study other diseases,[18],[19] seed-based correlation analysis was performed to obtain more information about specific differences in the functional connectivity of resting-state networks between RIS patients and healthy controls. We hypothesized that some resting-state neural networks involved in cognitive processes might be impaired in RIS patients, mainly the DMN and the central executive network.

METHODS

We initially recruited 27 RIS patients diagnosed according to Okuda et al.'s criteria [1] from MS databases of six Madrid (Spain) centers specializing in demyelinating diseases. Of these 27, two were excluded because of preprocessing problems of their MRIs. The final RIS sample consisted of 24 right-handed and one left-handed patient (21 women; mean age = 41.9 years). Reasons for the index RIS patient MRI, which was performed a mean of 5.3 years (range 0.5–16) earlier, were headache (N= 11), tinnitus-hypoacusis (N=5), cervicalgia (N=3), and miscellanea (N=6).

Neurologists with expertise in MS performed a thorough neurologic examination and an accurate clinical history to exclude any neurologic signs and history of remitting clinical symptoms lasting more than 24 hours consistent with MS. The patients also underwent a comprehensive workup to rule out other medical conditions that could explain the MRI-detected brain lesions.

Among the 25 RIS patients, 15 (60%) fulfilled the criteria for higher risk for conversion to future MS according to (a) the presence of lesions within the spinal cord or (b) no lesions of the spinal cord but the presence of at least two of the following characteristics: abnormal cerebrospinal fluid, gadolinium-enhancing lesions, or dissemination in time.[2] Among the 15 RIS patients classified as a higher risk for conversion to future MS, nine were based on spinal cord lesions criteria, and six were on several risk criteria. Table 1 summarizes the entire sample's demographic, clinical, and neuropsychological testing results and shows that the two groups did not differ in age, sex, and education.

We initially recruited 29 healthy controls from relatives or friends of health professionals at the University Hospital "12 de Octubre" and the University Hospital of Getafe in Madrid (Spain). However, one was excluded because of preprocessing problems with her MRI. The final sample of the control group was 26 right-handed and two left-handed healthy controls (23 women; mean age = 41.1 years). None of them had a history of known psychiatric or neurological disorders.

We excluded RIS patients and healthy controls with a history of alcohol or drug abuse, significant acute comorbidities, or any serious chronic illness (patients with stable chronic medical conditions were included).

After obtaining written (signed) informed consent from all participants, formal neuropsychological testing (see below) was implemented. In addition, on the same week of the neuropsychological testing, a multi-sequence MRI examination was acquired using a single 3 T scanner in a unique center, the Fuenlabrada University Hospital in Fuenlabrada, Madrid, Spain.

The ethical standards committee of the University Hospital "12 de Octubre" (Madrid, Spain) approved all procedures.

Cognitive functioning measurement

Intellectual abilities

Participants completed the Vocabulary and Matrix subtests from the Wechsler Adult Intelligence Scale–Third Edition (WAIS-III).[20] The vocabulary subtest was used as a traditional test of crystallized intellect influenced by educational experience, and the matrix subtest was used to measure fluid intelligence.[20] Both subtests tap into different cognitive domains, with vocabulary focusing on verbal comprehension and expression and matrix on nonverbal reasoning and problem-solving.[20]

Neuropsychological assessment

Cognitive functioning was performed through the Brief Repeatable Battery of Neuropsychological Tests.[21] We also administered the Stroop Color and Word Test, which aims to assess the phenomenon of interference linked to the inhibitory control process [22], and the Controlled Oral Word Association Test, which is used to explore phonemic fluency, executive functions, and memory.[23] The sequence of letters usually used and applied in this study was

"F," "A," and "S."[23] Depressive symptoms were assessed with Beck Depression Inventory–Second Edition.[24]

Each one of the neuropsychological test scores was converted to a z-score and adjusted for age, sex, and education, using the healthy controls as the reference group. First, age and education were centered around the mean (score - mean). Second, the coefficients for age, sex, and education, required to calculate expected test scores, were calculated using multiple linear regression analysis in healthy controls; the cognitive test scores (analyses were performed separately for each cognitive test) were the dependent variables, meanwhile age, sex, and education were the covariables. Third, expected test scores were computed for the entire group using a regression equation in which age, sex, and education were weighted by the estimated age, sex, and education regression coefficients generated previously. Finally, we calculated z-scores by dividing (actual test score - expected test score) by the standard deviation of the residuals. Failure of one test was defined as a z-score ≤ 1.5 standard deviations compared to healthy controls and cognitive impairment as a failure on at least two tests of different cognitive domains.[25]

MRI acquisition

Images were acquired in a General Electric HDxt 3T MR scanner, using a whole-body radio-frequency coil for signal excitation and a quadrature eight-channel coil for the reception. Structural images were obtained using a T1 weighted sequence (3D FSPGR T1-w: repetition time [TR] = 9,776 ms, echo time [TE] = 4,488 ms, inversion time [TI] = 450 ms, field of view= 288 mm, acquisition matrix = 288 × 288, slice thickness = 1 mm, full brain coverage,

resolution = 1 × 1 × 1 mm3, flip angle = 120; 170 sagittal slices). A fluid-attenuated inversion recovery (FLAIR) sequence (TR = 9002, TE= 150.852, TI = 2100, flip angle= 90, 30 slices, and thickness = 4 mm) was acquired to detect T2-hyperintense lesions.

Participants were instructed to keep their eyes closed, relax and not think about anything specific without falling asleep while acquiring resting-state fMRI data. These data were obtained using a gradient-echo echoplanar T2*-weighted sequence (240 volumes, 50 slices, TR = 2500 ms, TE = 16 ms, matrix dimensions = 64 x 64 pixels, voxel dimensions = 3.4 x 3.4 x 3 mm^3, flip angle = 77 and 4 dummy scans; total time = 8 min). Two Phase Encoding POLARity field map sequences with the same characteristics in opposite directions (posteroanterior and anterior-posterior) were acquired to correct magnetic susceptibility distortion.

Preprocessing

Visual inspection was carried out for the detection of artifacts and anatomical abnormalities. All volumes were manually reoriented. Preprocessing was performed using fMRIPrep 20.2.1. (available at https://fmriprep.org/en/stable/), one of the most reliable automated procedures providing optimal correction of magnetic susceptibility-induced distortions (phase-encoding polarity).[26],[27] This analysis included the following:

Anatomical data preprocessing: each T1-weighted (T1w) image was corrected for intensity non-uniformity with N4BiasFieldCorrection (ANTs 2.3.3) and used as a T1w-reference throughout the workflow. The T1w-reference was then skull-stripped with a Nipype implementation of the "antsBrainExtraction.sh"

workflow (from ANTs), using OASIS30ANTs as the target template. Brain tissue segmentation of cerebrospinal fluid, white matter, and gray matter was performed on the brain-extracted T1w using "fast" (FSL 5.0.9]. Volume-based spatial normalization to one standard space (MNI152NLin2009cAsym) was performed through nonlinear registration with "antsRegistration" (ANTs 2.3.3), using brain-extracted versions of both T1w reference and the T1w template.

Functional data preprocessing: a functional reference volume and its skull-stripped version were generated using a custom methodology of fMRIPrep. A B0-nonuniformity map (field map) was estimated based on two echo-planar imaging references with opposing phase-encoding directions, with "3dQwarp" (AFNI 20160207). The corrected echo-planar imaging reference was calculated based on the estimated susceptibility distortion for a more accurate co-registration with the anatomical reference. The BOLD reference was then co-registered to the T1w reference using "flirt" (FSL 5.0.9) with the boundary-based registration cost function. Co-registration was configured with nine degrees of freedom to account for distortions remaining in the BOLD reference. Head-motion parameters concerning the BOLD reference (transformation matrices and six corresponding rotation and translation parameters) were estimated before spatiotemporal filtering using "mcflirt" (FSL 5.0.9).

The BOLD time series were resampled onto their original, native space by applying a single composite transform to correct for head motion and susceptibility distortions. These resampled BOLD time series were resampled into a standard space. First, a reference volume and its skull-stripped version were generated using a custom methodology of fMRIPrep. Several confounding time series were calculated based on these data: framewise displacement,

DVARS, and three region-wise global signals. Framewise displacement was computed using Power (absolute sum of relative motions) and Jenkinson (relative root mean square displacement between affines). The three global signals were extracted within the cerebrospinal fluid, the white matter, and the whole-brain masks. Additionally, physiological regressors were removed for component-based noise correction.[28]

Structural data analysis

T2 hyperintense lesions were segmented in FLAIR images by employing the automated lesion growth algorithm as implemented in the Lesion Segmentation Toolbox (LST) version 2.0.1 (www.statisticalmodelling.de/lst.html) for Statistical Parametric Mapping (SPM12: http://www.fil.ion.ucl.ac.uk/spm).[29] Several studies have corroborated the validity of LST, also in MS studies [30]–[32]. Additionally, total and regional volumes (cortical and subcortical: caudate nucleus, putamen, globus pallidus, thalamus, amygdala, and hippocampus) were calculated using FreeSurfer v5.3.0 [33] freely available online (http://surfer.nmr.mgh.harvard.edu/). These measurements were normalized using the estimated intracranial volume provided by the software, which follows the procedure by Buckner et al.[34].

Functional connectivity analysis

The Conn Toolbox (available at https://www.nitrc.org/projects/conn), an open-source Matlab/SPM-based software, was used to perform the following analysis steps, given its high sensitivity and reliability in functional connectivity studies.[35] Independent Component Analysis (ICA) (Group-level ICA - RIS

patients and healthy controls -; the number of components = 25; dimensionality reduction = 64) provided spatial maps that were identified as the DMN, the sensorimotor network, the salience network, the dorsal attentional network, the frontoparietal network, the linguistic network, the cerebellum network, the central executive network, the medial visual network, and the lateral visual network. This identification was performed in CONN using the Sorensen-Dice coefficient to compare each map with the Human Connectome Project Independent Component Analysis atlas and visually complemented, following the procedure described in the literature.[18],[36],[37]. Additionally, seed-based correlation (SBC) analysis was used to gain more information about specific differences in the functional connectivity of resting-state networks between RIS patients and healthy controls, as previously done in the functional characterization of other diseases.[18],[19] The seeds of the resting-state networks used for this analysis are described in the Supplementary Material document.

Statistical Analyses

Statistical analyses for the clinical and neuropsychological measures were conducted using SPSS 21 (Statistical Package for the Social Sciences). We used two independent sample t-tests for continuous and normally distributed data) Moreover, the Mann–Whitney U test for nonnormally distributed data. Fisher's exact test was used to analyze group differences in sex.

A multivariate analysis of covariance (interest factor = group; covariates = sex and age) was used to explore intergroup differences (RIS vs. healthy

controls) in total volume, tissue volume, and regional volume measurements (cortical and subcortical). Because of the many statistical tests performed to compare neuropsychological z-scores and all these measurements, we used the Benjamini–Hochberg procedure with a defined false discovery rate of 5%.[38]

T2 lesion volume and the total number of T2-hyperintense brain lesions were compared between RIS patients and healthy controls using the Mann–Whitney U test as they were not normally distributed.

Intergroup differences in functional connectivity (ICA and SBC) were explored using the CONN toolbox. Specifically, we computed Pearson's correlation coefficients to conduct first-level functional connectivity analysis. The resulting correlation maps were then transformed into z-maps using Fisher's r-to-z transformation. Subsequently, these z-maps were incorporated into a general linear model analysis at the second level to perform between-group comparisons, using the false discovery rate (FDR) correction for multiple comparisons (RIS patients vs. healthy controls, covariates = sex and age; $p_{FDR} < 0.05$).

Using Pearson product-moment correlation coefficient or Spearman's rank correlation coefficient, when data were nonnormally distributed, we explored the correlations among the neuropsychological z-scores and the neuroimaging data (total and regional volume data, total number of T2-hyperintense brain lesions, T2 lesion volume, and functional connectivity data) whenever there were differences between groups.

Data Availability Statement

The data generated or analyzed during this study are available from the corresponding author upon reasonable request.

RESULTS

The 25 RIS patients did not differ from the 28 healthy controls regarding age, sex, and years of education (Table 1). However, in memory (verbal and visuospatial) and executive functions, RIS patients' cognitive performance was significantly worse than the healthy controls. In addition, fluid intelligence was also affected (Table 1). Sixteen out of 25 (64%) RIS patients failed at least one cognitive test, and nine (36.0%) fulfilled our criterion for cognitive impairment.

The T2 lesion volume (mL) (4.39 [2.21] ± 4.81 vs. 0.31 [0.15] ± 0.46; Mann-Whitney test, $p < 0.001$) and the total number of T2-hyperintense brain lesions (21.08 [20.50] ± 13.46 vs. 3.25 [3.0] ± 2.79; Mann-Whitney test, $p < 0.001$) were higher in the RIS patients compared to healthy controls (Table 1). On the other hand, using a multivariate analysis of covariance (interest factor = group; covariates = sex and age), there were no significant differences ($p < 0.05$) between the RIS and healthy control groups in brain total and regional volumes (cortical and subcortical).

The ICA intergroup comparisons (RIS patients vs. healthy controls; $p_{FDR} < 0.05$) of the identified resting-state neural networks showed significant results only in the DMN and the central executive network (Figure 1). The DMN presented higher connectivity with the right middle and the superior frontal gyri ($x = +32$, $y= +08$, $z = +58$) in RIS patients compared to healthy controls ($p_{FDR} = 0.023$) (Table 2). Significant intergroup differences were also observed in the

central executive network analysis: RIS patients showed higher connectivity of the central executive network with the thalamus (x = +14, y = -18, z = +06; p_{FDR} = 0.027) (Table 2). These networks showed no significant differences in the opposite contrast (healthy controls > RIS patients). No significant intergroup differences (RIS patients > healthy controls; healthy controls > RIS patients) existed in any other resting-state neural networks studied. The seed-based correlation analysis performed from each seed indicated above showed differences in functional connectivity in one anatomical region of the DMN, the posterior cingulate cortex (Table 2). Specifically, RIS patients presented higher functional connectivity than healthy controls (p_{FDR} = 0.034) between the posterior cingulate cortex and the precuneus (x = +06; y = -44; z = +60) (Figure 2) (Table 2).

A higher number of T2-hyperintense brain lesions was associated with poorer performance on neuropsychological tests, including memory (visual and visuospatial memory) and fluid intelligence in RIS patients (Table 3). Further, there was a significant correlation between T2 lesion volume and visuospatial memory (Table 3). On the other hand, there was no correlation between the neuropsychological tests and the functional connectivity data, except in the case of the delayed recall of the Selective Reminding Test (SRT) and the higher functional connectivity between the central executive network and the thalamus (Table 3). Indeed, the better scores in the delayed recall test from the SRT (verbal learning and memory), the higher functional connectivity between the central executive network and the thalamus.

DISCUSSION

In this study, we have detected alterations in the functional connectivity of resting-state neural networks in RIS patients. Compared to healthy controls, RIS patients showed higher functional connectivity between the DMN and the middle and superior frontal gyri and between the central executive network and the thalamus ($p_{FDR} < 0.05$; corrected). In addition, the seed-based correlation analysis revealed that RIS patients presented higher functional connectivity of the posterior cingulate cortex, an important hub in neural networks, and the precuneus. Interestingly, only the correlation between RIS patients' neuropsychological performance in delayed recall (verbal learning and memory) and the functional connectivity between the central executive network with the thalamus was significant. This positive correlation suggests that higher functional connectivity in the central executive network with the thalamus may be associated with successfully consolidating and retaining information over time in RIS patients because of a compensatory brain mechanism (see below). Indeed, RIS patients and healthy controls did not show significant differences in their performance on this specific test (Table 1).

Regarding anatomical data, contrary to other studies,[3],[8] we did not find statistically significant differences in brain volume between RIS patients and the healthy control group. The volumetric analysis of various brain regions, including the thalamus, yielded no significant variations between the two groups. Importantly, the total number of T2-hyperintense brain lesions was associated with greater impairment in memory (visual and visuospatial memory) and fluid intelligence, suggesting that the damage or disruption caused by these

lesions in specific brain regions can impact the cognitive functioning of RIS patients (Table 2).

The higher connectivity appears contradictory at first glance but has been observed in several other conditions, such as cognitive impairment, clinically isolated syndrome, diabetes mellitus, essential tremor, and orthostatic tremor.[14],[15],[39]–[41] Two possible mechanisms may partly explain how network dynamics interrelate in RIS. First, resting-state neural networks are functionally interconnected, and a malfunction in one network may cause a malfunction in others.[42],[43] As RIS patients may exhibit cognitive deficits [5],[11]–[13], it is not surprising to find altered resting-state neural networks involved in cognitive processes. Increased functional connectivity may reflect changes in neuronal activity, becoming more congruent between regions [44] and indicating a compensatory brain mechanism for early neuronal dysfunction.[45] The capacity may be lost as neuronal dysfunction advances, decreasing connectivity.[44] This theory may explain the observed higher connectivity in RIS patients presented here. As RIS progresses (i.e., the development of MS), neuronal dysfunction will likely be significantly more prominent. In contrast, the more relatively preserved neurons in RIS may be able to provide a more effective compensatory mechanism. Of interest is that DMN and the central executive network may also be involved in MS.[46],[47] However, in MS, alterations of resting-state neural networks are widespread and associated with motor, sensory, visual, and cognitive function abnormalities.[48] Second, increased connectivity may not be compensatory but rather reflect abnormal neural activity or circuitry due to pathological processes like microglia-induced inflammation, contributing to aberrant neural

plasticity.[43] The increased connectivity, whether compensatory or maladaptive, may finally contribute to cognitive deficits. Notwithstanding, further research is needed to elucidate the mechanisms of network reorganization and their relationship to physical and cognitive disability in RIS.

The neuropsychological profile of RIS patients is generally similar to that of MS.[11],[12] Two studies in RIS found a higher frequency of cognitive deficits with the same neuropsychological profile as patients with established relapsing-remitting MS.[11],[12] A study comparing RIS vs. clinically isolated syndrome, i.e., the earliest stage of relapsing-remitting MS, has shown that 21.4% of RIS patients suffered cognitive impairment, a proportion virtually identical to that observed in clinically isolated syndrome patients.[13] Our patients performed worse than the healthy controls, in different cognitive areas, mainly in verbal and visuospatial memory and executive functions. Of interest was that fluid intelligence was affected in RIS patients. This latter finding has also been reported in MS and could play a role in altering executive deficits.[49]

To our knowledge, only one study has investigated functional connectivity in RIS patients.[17] In that study,[17] no differences in functional brain connectivity were found between RIS subjects and healthy controls. The possible explanations for these discrepant results are a) the heterogeneity of RIS patients regarding disease duration/characteristics and b) methodological issues, such as MRI data acquisition and preprocessing, and the different approaches used to explore functional connectivity and intergroup differences. Specifically, our MRI data were based on more recent acquisition and analysis methods, including correction for magnetic susceptibility and optimal physiological denoising.

The study should be interpreted within the context of several limitations. First, the sample size was relatively small. However, given the low incidence and prevalence of the disease, the RIS neuroimaging literature generally comprises studies with small sample sizes. Second, we recruited a group of RIS patients from the clinics of six different hospitals, and therefore, our results might not be generalized to population-dwelling RIS patients. However, the proportion of RIS patients at high risk for conversion to MS (15/25) is similar to that of RIS patients who developed MS within ten years in a recent large longitudinal study,[7] indicating that our sample may be representative of the general population with RIS. Third, the study's cross-sectional design could be viewed as a snapshot of a condition at a given time. Finally, we decided not to apply lesion filling, a controversial procedure given the difficulties observed in automatic segmentation, and that led some authors to suggest caution when choosing this approach, especially in individuals with higher lesions loads.[50] Specifically, the filled regions may not fully replicate the original data, which can introduce artifacts and inaccuracies, potentially affecting the identification of functional connectivity networks and the posterior statistical analysis.[50]

In closing, our results indicate the existence of aberrant connectivity in RIS patients, suggesting that brain tissue damage may not be limited to focal white matter lesions. Our RIS patients had abnormal brain connectivity in major resting-state neural networks that might be involved in non-motor symptoms (i.e., cognitive features). These findings support the hypothesis that RIS should be considered not an "incidental finding", but an exclusively non-motor (neurocognitive) variant of MS. Further research with larger sample sizes is

required to comprehend better the pathophysiological processes underlying this novel entity.

Acknowledgments: J. Benito-León is supported by the National Institutes of Health, Bethesda, MD, USA (NINDS #R01 NS39422), the European Commission (grant ICT-2011-287739, NeuroTREMOR), the Ministry of Economy and Competitiveness (grant RTC-2015-3967-1, NetMD—platform for the tracking of movement disorder), and the Spanish Health Research Agency (grant FIS PI12/01602 and grant FIS PI16/00451).

Disclosures:

Julián Benito-León (jbenitol67@gmail.com) reports no relevant disclosures.

Ana Belén del Pino (ab.delpino@alumnos.urjc.es) reports no relevant disclosures.

Yolanda Aladro (yolanda.aladro@salud.madrid.org) reports no relevant disclosures.

Constanza Cuevas (constanzaece@gmail.com) reports no relevant disclosures.

Ángela Domingo-Santos (angeladomingosantos@gmail.com) reports no relevant disclosures.

Victoria Galán Sánchez-Seco (vickyg_s@hotmail.com) reports no relevant disclosures.

Andrés Labiano-Fontcuberta (gandilabiano@hotmail.com) reports no relevant disclosures.

Ana Gómez López (anagmlp@gmail.com) reports no relevant disclosures.

Paula Salgado-Cámara (paula.salgado.camara@gmail.com) reports no relevant disclosures.

Lucienne Costa-Frossard (lufrossard@yahoo.es) reports no relevant disclosures.

Enrique Monreal (enrique.monreal@salud.madrid.org) reports no relevant disclosures.

Susana Sainz de la Maza (susana.sainzdelamaza@salud.madrid.org) reports no relevant disclosures.

Jordi A. Matias-Guiu (jordimatiasguiu@hotmail.com) reports no relevant disclosures.

Jorge Matias-Guiu (matiasguiu@gmail.com) reports no relevant disclosures.

Alfonso Delgado-Álvarez (alfonso.delgado.alvarez@hotmail.com) reports no relevant disclosures.

Paloma Montero-Escribano (pmontero84@gmail.com) reports no relevant disclosures.

Mª Luisa Martínez-Ginés (marisamgines@hotmail.com) reports no relevant disclosures.

Yolanda Higueras (yolandahigueras@googlemail.com) reports no relevant disclosures.

Lucía Ayuso-Peralta (layusoperalta@gmail.com) reports no relevant disclosures.

Norberto Malpica (norberto.malpica@urjc.es) reports no relevant disclosures.

Helena Melero (hmelero@ucm.es) reports no relevant disclosures.

Author contributions

Julián Benito-León collaborated with 1) the conception, organization, and execution of the research project; 2) the statistical analysis design; and; 3) the writing of the manuscript's first draft and the review and critique.

Ana Belén del Pino collaborated with 1) the conception, organization, and execution of the research project; 2) MRI data analysis 3) the statistical analysis

design; and; 4) the writing of the manuscript's first draft and the review and critique.

Yolanda Aladro collaborated with 1) the conception, organization, and execution of the research project; and 2) the review and critique.

Constanza Cuevas collaborated with 1) the conception, organization, and execution of the research project; and 2) the review and critique.

Ángela Domingo-Santos collaborated with 1) the conception, organization, and execution of the research project; and 2) the review and critique.

Victoria Galán Sánchez-Seco collaborated with 1) the conception, organization, and execution of the research project; and 2) the review and critique.

Andrés Labiano-Fontcuberta collaborated with 1) the conception, organization, and execution of the research project; and 2) the review and critique.

Ana Gómez López collaborated with 1) the conception, organization, and execution of the research project; and 2) the review and critique.

Paula Salgado-Cámara collaborated with 1) the conception, organization, and execution of the research project; and 2) the review and critique.

Lucienne Costa-Frossard collaborated with 1) the conception, organization, and execution of the research project; and 2) the review and critique.

Enrique Monreal collaborated with 1) the conception, organization, and execution of the research project; and 2) the review and critique.

Susana Sainz de la Maza collaborated with 1) the conception, organization, and execution of the research project; and 2) the review and critique.

Jordi A. Matias-Guiu collaborated with 1) the conception, organization, and execution of the research project; and 2) the review and critique.

Jorge Matias-Guiu Guia collaborated with 1) the conception, organization, and execution of the research project; and 2) the review and critique.

Alfonso Delgado-Álvarez collaborated with 1) the conception, organization, and execution of the research project; and 2) the review and critique.

Paloma Montero-Escribano collaborated with 1) the conception, organization, and execution of the research project; and 2) the review and critique.

Mª Luisa Martínez Ginés collaborated with 1) the conception, organization, and execution of the research project; and 2) the review and critique.

Yolanda Higueras collaborated with 1) the conception, organization, and execution of the research project; and 2) the review and critique.

Lucía Ayuso-Peralta collaborated with 1) the conception, organization, and execution of the research project; and 2) the review and critique.

Norberto Malpica collaborated with 1) the conception, organization, and execution of the research project; and 2) the review and critique.

Helena Melero collaborated with 1) the conception, organization, and execution of the research project; 2) MRI data analysis; 3) the statistical analysis design; and; 4) the writing of the manuscript's first draft and the review and critique.

REFERENCES

1. **Okuda DT, Mowry EM, Beheshtian A, *et al.*** Incidental MRI anomalies suggestive of multiple sclerosis: The radiologically isolated syndrome. *Neurology*. 2009; **72**(9):800–805. Available at: https://www.neurology.org/lookup/doi/10.1212/01.wnl.0000335764.14513.1a [Accessed July 8, 2023].

2. **Labiano-Fontcuberta A, Mato-Abad V, Álvarez-Linera J, *et al.*** Normal-appearing brain tissue analysis in radiologically isolated syndrome using 3 T MRI. *Medicine*. 2016; **95**(27):e4101. Available at: https://journals.lww.com/00005792-201607050-00052 [Accessed November 13, 2022].

3. **Labiano-Fontcuberta A, Mato-Abad V, Álvarez-Linera J, *et al.*** Gray Matter Involvement in Radiologically Isolated Syndrome. *Medicine*. 2016; **95**(13):e3208. Available at: https://journals.lww.com/00005792-201603290-00019 [Accessed November 13, 2022].

4. **Mato-Abad V, Labiano-Fontcuberta A, Rodríguez-Yáñez S, *et al.*** Classification of radiologically isolated syndrome and clinically isolated syndrome with machine-learning techniques. *Eur J Neurol*. 2019; **26**(7):1000–1005. Available at: https://onlinelibrary.wiley.com/doi/10.1111/ene.13923 [Accessed November 13, 2022].

5. **Domingo-Santos Á, Labiano-Fontcuberta A, Aladro-Benito Y, *et al.*** Predicting conversion to multiple sclerosis by assessing cognitive impairment in radiologically isolated syndrome. *Multiple Sclerosis and Related Disorders*. 2021; **49**:102749. Available at: https://linkinghub.elsevier.com/retrieve/pii/S2211034821000158 [Accessed August 15, 2022].

6. **Labiano-Fontcuberta A**, **Benito-León J**. Radiologically isolated syndrome: An update on a rare entity. *Mult Scler*. 2016; **22**(12):1514–1521. Available at: http://journals.sagepub.com/doi/10.1177/1352458516653666 [Accessed July 8, 2023].

7. **Lebrun-Frenay C, Kantarci O, Siva A, *et al.*** Radiologically Isolated Syndrome: 10-YEAR Risk Estimate of a Clinical Event. *Annals of Neurology*. 2020; **88**(2):407–417. Available at: https://onlinelibrary.wiley.com/doi/10.1002/ana.25799 [Accessed November 13, 2022].

8. **Azevedo CJ, Overton E, Khadka S, *et al.*** Early CNS neurodegeneration in radiologically isolated syndrome. *Neurol Neuroimmunol Neuroinflamm*. 2015; **2**(3):e102. Available at: http://nn.neurology.org/lookup/doi/10.1212/NXI.0000000000000102 [Accessed February 26, 2023].

9. **Van Der Werf YD, Tisserand DJ, Visser PJ, *et al.*** Thalamic volume predicts performance on tests of cognitive speed and decreases in healthy aging. *Cognitive Brain Research*. 2001; **11**(3):377–385. Available at:

https://linkinghub.elsevier.com/retrieve/pii/S0926641001000106 [Accessed February 26, 2023].

10. **Labiano-Fontcuberta A, Aladro Y, Martínez-Ginés ML, *et al.*** Psychiatric disturbances in radiologically isolated syndrome. *Journal of Psychiatric Research*. 2015; **68**:309–315. Available at: https://linkinghub.elsevier.com/retrieve/pii/S0022395615001491 [Accessed July 8, 2023].

11. **Lebrun C, Blanc F, Brassat D, *et al.*** Cognitive function in radiologically isolated syndrome. *Mult Scler*. 2010; **16**(8):919–925. Available at: http://journals.sagepub.com/doi/10.1177/1352458510375707 [Accessed August 15, 2022].

12. **Amato MP, Hakiki B, Goretti B, *et al.*** Association of MRI metrics and cognitive impairment in radiologically isolated syndromes. *Neurology*. 2012; **78**(5):309–314. Available at: https://www.neurology.org/lookup/doi/10.1212/WNL.0b013e31824528c9 [Accessed November 28, 2022].

13. **Labiano-Fontcuberta A, Martínez-Ginés ML, Aladro Y, *et al.*** A comparison study of cognitive deficits in radiologically and clinically isolated syndromes. *Mult Scler*. 2016; **22**(2):250–253. Available at: http://journals.sagepub.com/doi/10.1177/1352458515591072 [Accessed July 9, 2023].

14. **Benito-León J, Louis ED, Romero JP, *et al.*** Altered Functional Connectivity in Essential Tremor: A Resting-State fMRI Study. *Medicine*. 2015; **94**(49):e1936. Available at: https://journals.lww.com/00005792-201512080-00005 [Accessed July 9, 2023].

15. **Benito-León J, Louis ED, Manzanedo E, *et al.*** Resting state functional MRI reveals abnormal network connectivity in orthostatic tremor. *Medicine*. 2016; **95**(29):e4310. Available at: https://journals.lww.com/00005792-201607190-00048 [Accessed November 13, 2022].

16. **Benito-León J, Sanz-Morales E, Melero H, *et al.*** Graph theory analysis of resting-state functional magnetic resonance imaging in essential tremor. *Hum Brain Mapp*. 2019; **40**(16):4686–4702. Available at: https://onlinelibrary.wiley.com/doi/10.1002/hbm.24730 [Accessed July 9, 2023].

17. **Giorgio A, Stromillo ML, De Leucio A, *et al.*** Appraisal of Brain Connectivity in Radiologically Isolated Syndrome by Modeling Imaging Measures. *J. Neurosci.* 2015; **35**(2):550–558. Available at: https://www.jneurosci.org/lookup/doi/10.1523/JNEUROSCI.2557-14.2015 [Accessed July 9, 2023].

18. **Soman SM, Raghavan S, Rajesh PG, *et al.*** Does resting state functional connectivity differ between mild cognitive impairment and early Alzheimer's dementia? *Journal of the Neurological Sciences*. 2020; **418**(1):1–8.

19. **Yu Y**, **He L**. Group-ICA with Functional Connectivity During Inhibition Control in Young Adults With Autistic-like Traits: an fMRI Study of a Stop-Signal Task. *Research Square*. 2020; **10**(1):1–26.

20. **Kaufman AS**, **Lichtenberger EO**. *Essentials of WAIS-III assessment.* Hoboken, NJ, US: John Wiley & Sons Inc; 1999:viii, 260.

21. **Rao SM**. A manual for the brief repeatable battery of neuropsychological tests in multiple sclerosis. *Milwaukee: Medical College of Wisconsin*. 1990; **1696**.

22. **Scarpina F**, **Tagini S**. The Stroop Color and Word Test. *Front. Psychol.* 2017; **8**. Available at: http://journal.frontiersin.org/article/10.3389/fpsyg.2017.00557/full [Accessed October 28, 2022].

23. **Bauer K**, **Malek-Ahmadi M**. Meta-analysis of Controlled Oral Word Association Test (COWAT) FAS performance in amnestic mild cognitive impairment and cognitively unimpaired older adults. *Applied Neuropsychology: Adult*. 2021:1–7. Available at: https://www.tandfonline.com/doi/full/10.1080/23279095.2021.1952590 [Accessed October 28, 2022].

24. **Beck AT**. An Inventory for Measuring Depression. *Arch Gen Psychiatry*. 1961; **4**(6):561. Available at: http://archpsyc.jamanetwork.com/article.aspx?doi=10.1001/archpsyc.1961.01710120031004 [Accessed October 28, 2022].

25. **McKhann G, Drachman D, Folstein M, *et al.*** Clinical diagnosis of Alzheimer's disease: report of the NINCDS-ADRDA Work Group under the auspices of Department of Health and Human Services Task Force on Alzheimer's Disease. *Neurology*. 1984; **34**(7):939–944.

26. **Esteban O, Markiewicz CJ, Blair RW, *et al.*** fMRIPrep: a robust preprocessing pipeline for functional MRI. *Nature methods*. 2019; **16**(1):111–116.

27. **Esteban O, Ciric R, Finc K, *et al.*** fMRIPrep: a robust preprocessing pipeline for functional MRI. *Nature Protocols*. 2020; **15**(1):2186–2202.

28. **Behzadi Y**, **Restom K**, **Liau J**, **Liu TT**. A component based noise correction method (CompCor) for BOLD and perfusion based fMRI. *NeuroImage*. 2007; **37**(1):90–101. Available at: https://linkinghub.elsevier.com/retrieve/pii/S1053811907003837 [Accessed July 8, 2023].

29. **Schmidt P, Gaser C, Arsic M, *et al.*** An automated tool for detection of FLAIR-hyperintense white-matter lesions in Multiple Sclerosis. *NeuroImage*. 2012; **59**(4):3774–3783. Available at: https://linkinghub.elsevier.com/retrieve/pii/S1053811911013139 [Accessed April 20, 2023].

30. **Valverde S, Oliver A, Roura E, *et al.*** Quantifying brain tissue volume in multiple sclerosis with automated lesion segmentation and filling. *NeuroImage: Clinical*. 2015;

9:640–647. Available at: https://linkinghub.elsevier.com/retrieve/pii/S2213158215300127 [Accessed April 20, 2023].

31. **Pareto D, Sastre-Garriga J, Aymerich FX, *et al.*** Lesion filling effect in regional brain volume estimations: a study in multiple sclerosis patients with low lesion load. *Neuroradiology*. 2016; **58**(5):467–474. Available at: http://link.springer.com/10.1007/s00234-016-1654-5 [Accessed April 20, 2023].

32. **Biberacher V, Schmidt P, Keshavan A, *et al.*** Intra- and interscanner variability of magnetic resonance imaging based volumetry in multiple sclerosis. *NeuroImage*. 2016; **142**:188–197. Available at: https://linkinghub.elsevier.com/retrieve/pii/S1053811916303421 [Accessed April 20, 2023].

33. **Fischl B**, **Dale AM**. Measuring the thickness of the human cerebral cortex from magnetic resonance images. *Proc. Natl. Acad. Sci. U.S.A.* 2000; **97**(20):11050–11055. Available at: https://pnas.org/doi/full/10.1073/pnas.200033797 [Accessed April 20, 2023].

34. **Buckner RL, Head D, Parker J, *et al.*** A unified approach for morphometric and functional data analysis in young, old, and demented adults using automated atlas-based head size normalization: reliability and validation against manual measurement of total intracranial volume. *NeuroImage*. 2004; **23**(2):724–738. Available at: https://linkinghub.elsevier.com/retrieve/pii/S1053811904003271 [Accessed July 8, 2023].

35. **Whitfield-Gabrieli S**, **Nieto-Castanon A**. Conn: a functional connectivity toolbox for correlated and anticorrelated brain networks. *Brain connectivity*. 2012; **2**(3):125–141.

36. **Beckmann CF**, **DeLuca M**, **Devlin JT**, **Smith SM**. Investigations into resting-state connectivity using independent component analysis. *Phil. Trans. R. Soc. B*. 2005; **360**(1457):1001–1013. Available at: https://royalsocietypublishing.org/doi/10.1098/rstb.2005.1634 [Accessed April 2, 2023].

37. **Kelly RE, Wang Z, Alexopoulos GS, *et al.*** Hybrid ICA-Seed-Based Methods for fMRI Functional Connectivity Assessment: A Feasibility Study. *International Journal of Biomedical Imaging*. 2010; **2010**:1–24. Available at: http://www.hindawi.com/journals/ijbi/2010/868976/ [Accessed April 2, 2023].

38. **Benjamini Y**, **Hochberg Y**. Controlling the False Discovery Rate: A Practical and Powerful Approach to Multiple Testing. *Journal of the Royal Statistical Society. Series B (Methodological)*. 1995; **57**(1):289–300. Available at: http://www.jstor.org/stable/2346101 [Accessed June 28, 2021].

39. **Celone KA, Calhoun VD, Dickerson BC, *et al.*** Alterations in Memory Networks in Mild Cognitive Impairment and Alzheimer's Disease: An Independent Component Analysis. *Journal of Neuroscience*. 2006; **26**(40):10222–10231. Available at:

https://www.jneurosci.org/lookup/doi/10.1523/JNEUROSCI.2250-06.2006 [Accessed November 13, 2022].

40. **Roosendaal SD, Schoonheim MM, Hulst HE, *et al.*** Resting state networks change in clinically isolated syndrome. *Brain*. 2010; **133**(6):1612–1621. Available at: https://academic.oup.com/brain/article-lookup/doi/10.1093/brain/awq058 [Accessed November 13, 2022].

41. **van Duinkerken E, Schoonheim MM, Sanz-Arigita EJ, *et al.*** Resting-state brain networks in type 1 diabetic patients with and without microangiopathy and their relation to cognitive functions and disease variables. *Diabetes*. 2012; **61**(7):1814–1821.

42. **Widjaja E**, **Zamyadi M**, **Raybaud C**, **Snead OC**, **Smith ML**. Abnormal functional network connectivity among resting-state networks in children with frontal lobe epilepsy. *AJNR Am J Neuroradiol*. 2013; **34**(12):2386–2392.

43. **Groppa S**, **Gonzalez-Escamilla G**, **Eshaghi A**, **Meuth SG**, **Ciccarelli O**. Linking immune-mediated damage to neurodegeneration in multiple sclerosis: could network-based MRI help? *Brain Communications*. 2021; **3**(4):fcab237. Available at: https://academic.oup.com/braincomms/article/doi/10.1093/braincomms/fcab237/6383135 [Accessed June 11, 2023].

44. **Meijboom R, Steketee RME, de Koning I, *et al.*** Functional connectivity and microstructural white matter changes in phenocopy frontotemporal dementia. *Eur Radiol*. 2017; **27**(4):1352–1360. Available at: http://link.springer.com/10.1007/s00330-016-4490-4 [Accessed November 30, 2022].

45. **Borroni B, Alberici A, Cercignani M, *et al.*** Granulin mutation drives brain damage and reorganization from preclinical to symptomatic FTLD. *Neurobiology of Aging*. 2012; **33**(10):2506–2520. Available at: https://linkinghub.elsevier.com/retrieve/pii/S0197458011004623 [Accessed November 30, 2022].

46. **Rocca MA, Valsasina P, Martinelli V, *et al.*** Large-scale neuronal network dysfunction in relapsing-remitting multiple sclerosis. *Neurology*. 2012; **79**(14):1449–1457. Available at: https://www.neurology.org/lookup/doi/10.1212/WNL.0b013e31826d5f10 [Accessed November 13, 2022].

47. **Bonavita S, Sacco R, Esposito S, *et al.*** Default mode network changes in multiple sclerosis: a link between depression and cognitive impairment? *Eur J Neurol*. 2017; **24**(1):27–36. Available at: https://onlinelibrary.wiley.com/doi/10.1111/ene.13112 [Accessed November 13, 2022].

48. **Sbardella E**, **Petsas N**, **Tona F**, **Pantano P**. Resting-State fMRI in MS: General Concepts and Brief Overview of Its Application. *BioMed Research International*. 2015; **2015**:1–8. Available at: http://www.hindawi.com/journals/bmri/2015/212693/ [Accessed November 30, 2022].

49. **Goitia B, Bruno D, Abrevaya S, *et al.*** The relationship between executive functions and fluid intelligence in multiple sclerosis Bergsland N, ed. *PLoS ONE*. 2020; **15**(4):e0231868. Available at: https://dx.plos.org/10.1371/journal.pone.0231868 [Accessed November 14, 2022].

50. **van der Weijden CWJ, Pitombeira MS, Haveman YRA, *et al.*** The effect of lesion filling on brain network analysis in multiple sclerosis using structural magnetic resonance imaging. *Insights Imaging*. 2022; **13**(1):63.

FIGURE LEGENDS:

FIGURE 1: Results of the independent component analysis. RIS patients showed higher functional connectivity than healthy controls; pFDR < 0.05 in default mode network (A) and central executive network (B). For visualization reasons, results are show with a significance level of 0.008 (uncorrected).

FIGURE 2: Results of seed-based correlation analysis. RIS patients showed higher functional connectivity than healthy controls between the posterior cingulate cortex and the precuneus; pFDR < 0.05). For visualization reasons, results are shown at a significance level of 0.008 (uncorrected).

Table 1. Demographic, Clinical, Laboratory, Conventional Neuroimaging, and Neuropsychological evaluation data.

	Radiologically isolated syndrome patients (N = 25)	**Healthy controls (N = 28)**	**p-value**
DEMOGRAPHIC VARIABLES			
Age in years	41.9 (42.0) ± 8.8	41.1 (43.5) ± 8.0	0.725 [a]
Sex (women)	21 (84.0%)	23 (82.1%)	1.0 [b]
Years of education	14.5 (15.0) ± 3.7	15.1 (15.0) ± 2.1	0.667 [c]
CLINICAL, LABORATORY AND CONVENTIONAL NEUROIMAGING VARIABLES			
Mean age at radiologically isolated syndrome diagnosis	36.3 (36.0) ± 9.3	-	-
Spinal cord lesions on magnetic resonance imaging	9 (36.0%)	-	
T2 lesion volume (mL)	4.39 (2.21) ± 4.81	0.31 (0.15) ± 0.46	**<0.001** [c]
Total number of T2-hyperintense brain lesions	21.08 (20.50) ± 13.46	3.25 (3.0) ± 2.79	**<0.001** [c]
Presence of oligoclonal bands and abnormal IgG index	13 (52.0%)	-	
Dissemination in time criteria	9 (36.0%)	-	
Gadolinium enhancing lesions	4 (16.0%)	-	
NEUROPSYCHOLOGICAL EVALUATION (STANDARDIZED TEST SCORES)			
INTELLECTUAL ABILITIES			
Vocabulary from the Wechsler Adult Intelligence Scale-Third Edition	0.00 ± 1.13	0.00 ± 1.00	0.984 [a]
Matrix subtest from the Wechsler Adult Intelligence Scale-Third Edition	-1.31 ± 1.93	0.00 ± 1.00	**0.048** [c]
VERBAL MEMORY			
Selective Reminding Test			
Long-term storage	-0.02 ± 0.14	0.00 ± 1.00	0.520 [c]
Consistent Long Term Retrieval	-0.70 ± 0.99	0.00 ± 1.00	**0.048** [a]
Delayed Recall	-0.66 ± 1.35	-0.04 ± 0.97	0.191 [c]
VISUOSPATIAL MEMORY			
10/36 Spatial Recall Test			
Immediate Recall	-0.81 ± 0.85	0.00 ± 1.00	**0.039** [a]
Delayed Recall	-0.56 ± 0.88	0.00 ± 1.00	0.075 [c]
ATTENTION AND PROCESSING SPEED			
Paced Auditory Serial Addition Test-3 seconds	0.06 ± 0.54	0.09 ± 0.34	0.191 [c]
Symbol Digit Modalities Test	-0.45 ± 0.76	0.00 ± 1.00	0.167 [a]
EXECUTIVE FUNCTIONS			
Word List Generation	-0.70 ± 0.98	0.00 ± 1.00	**0.048** [a]
Controlled Oral Word Association Test	-0.36 ± 1.24	0.00 ± 1.00	0.330 [a]

Stroop Color-Word Trial	-0.44 ± 0.90	0.00 ± 1.00	0.191 [a]
DEPRESSION SYMPTOMS			
Beck Depression Inventory–Second Edition	0.60 ± 1.68	0.00 ± 1.00	0.336 [c]

[a] Student's t-test; [b] Fisher's exact test; [c] Mann-Whitney test. Mean ± standard deviation (median) and frequency (%) are reported. Significant differences in the neuropsychological test z-scores have been corrected for familywise error rate with the Benjamini–Hochberg procedure, with a defined % false discovery rate of 5%. Significant values are in bold.

Table 2. Intergroup differences in functional connectivity (RIS patients > healthy controls; $p_{FDR} < 0.05$; Independent Component Analysis and Seed-Based Correlation results)

Independent Component Analysis Results				
Resting-state neural networks	Regions of Interest	Cluster size (vx)	Montreal Neurological Institute coordinates x y z	p-value (FDR corrected)
Default Mode Network	Middle frontal gyrus Superior frontal gyrus	18 10	32 8 58	0.023
Executive Control Network	Thalamus	26	14 -18 6	0.027
Seed-Based Correlation Analysis Results				
Seed region	Regions of Interest	Cluster size (vx)	Montreal Neurological Institute coordinates x y z	p-value (FDR corrected)
Posterior cingulate cortex	Precuneus	21	6 -44 60	0.034

Table 3. Matrix of correlations between the z-scores of all neuropsychological tests and the total T2-hyperintense brain lesions, T2 lesion volume, and functional connectivity data in RIS patients.

	Total number of T2-hyperintense brain lesions	T2 lesion volume	Default mode network (connectivity with the right middle and the superior frontal gyri)	Central executive network (connectivity with the thalamus)	Seed-based correlation analysis (connectivity of the posterior cingulate cortex)
INTELLECTUAL ABILITIES					
Vocabulary from the Wechsler Adult Intelligence Scale-Third Edition	-0.097 [a]	0.097 [b]	-0.144 [a]	0.204 [b]	0.066 [b]
Matrix subtest from the Wechsler Adult Intelligence Scale-Third Edition	**-0.456** [* a]	-0.104 [b]	-0.361 [a]	-0.135 [b]	-0.157 [b]
VERBAL LEARNING AND MEMORY					
Selective Reminding Test					
Long-term storage	-0.005 [b]	0.159 [b]	-0.056 [b]	-0.080 [b]	-0.051 [b]
Consistent Long Term Retrieval	-0.325 [a]	-0.333 [b]	0.258 [a]	0.258 [b]	0.093 [b]
Delayed Recall	**-0.505** [* b]	-0.367 [b]	0.336 [b]	**0.418** [* b]	0.052 [b]
VISUOSPATIAL MEMORY					
10/36 Spatial Recall Test					
Immediate Recall	**-0.482** [* a]	**-0.444** [* b]	-0.058 [a]	0.103 [b]	-0.083 [b]
Delayed Recall	**-0.506** [* a]	**-0.541** [** b]	0.090 [a]	0.191 [b]	-0.139 [b]
ATTENTION AND PROCESSING SPEED					
Paced Auditory Serial Addition Test-3 seconds	-0.036 [b]	-0.084 [b]	-0.263 [b]	0.235 [b]	-0.095 [b]
Symbol Digit Modalities Test	-0.381 [a]	-0.231 [b]	-0.144 [a]	-0.057 [b]	0.067 [b]
EXECUTIVE FUNCTIONS					
Word List Generation	-0.137 [a]	0.007 [b]	0.118 [a]	0.292 [b]	0.148 [b]
Controlled Oral Word Association Test	-0.220 [a]	-0.155 [b]	0.140 [a]	0.347 [b]	-0.074 [b]
Stroop Color-Word Trial	-0.253 [a]	-0.167 [b]	0.031 [a]	0.207 [b]	0.010 [b]
DEPRESSION SYMPTOMS					
Beck Depression Inventory–Second Edition	0.081 [b]	-0.029 [b]	0.268 [b]	0.060 [b]	-0.040 [b]

[a] Pearson product-moment correlation coefficient. [b] Spearman rank correlation coefficients. [*] $p < 0.05$; [**] $p < 0.01$. Significant values are in bold.

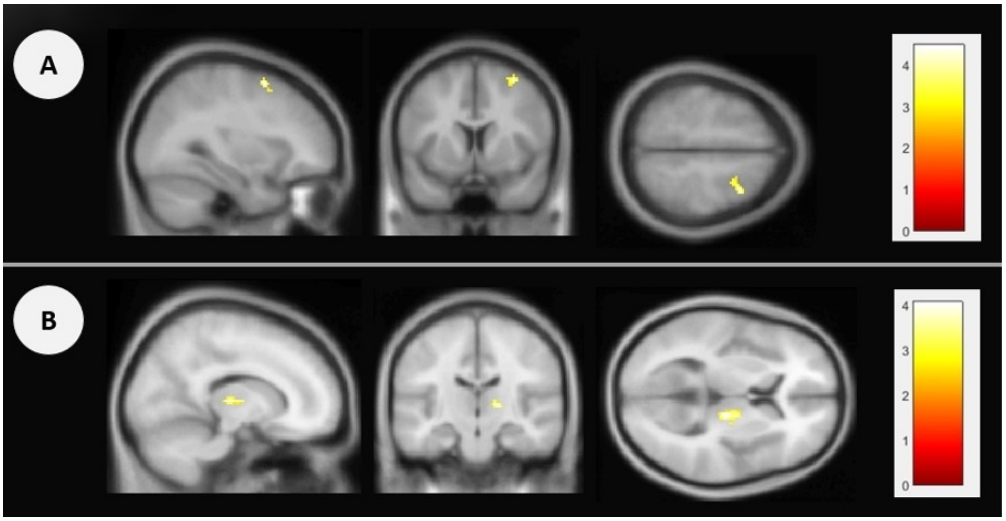

Figure 1. Results of the independent component analysis. RIS patients showed higher functional connectivity than healthy controls; pFDR < 0.05 in default mode network (A) and central executive network (B). For visualization reasons, results are shown with a significance level of 0.008 (uncorrected).

159x81mm (144 x 144 DPI)

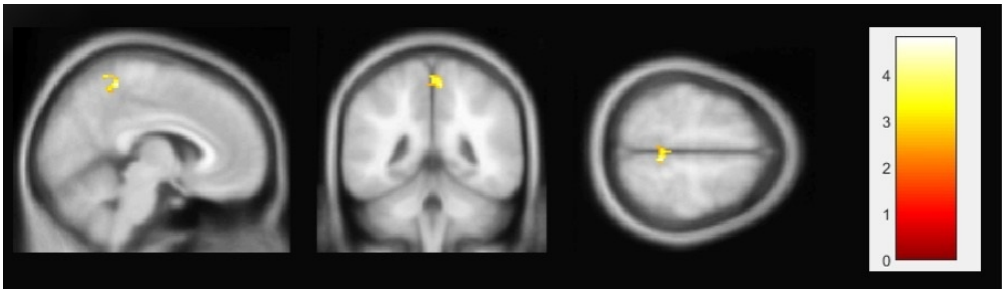

Figure 2. Results of the seed-based correlation analysis. RIS patients showed higher functional connectivity than healthy controls; pFDR < 0.05). For visualization reasons, results are shown at a significance level of 0.008 (uncorrected).

159x45mm (144 x 144 DPI)

SUPPLEMENTARY MATERIAL

Regions used in the seed-based correlation analysis (MNI coordinates)

Seed Region	X	Y	Z
Ventromedial prefrontal cortex of the default mode network	+1	+55	-3
Lateral parietal cortex of the default mode network (left)	-39	-77	+33
Lateral parietal cortex of the default mode network (right)	+47	-67	-29
Posterior cingulate cortex of the default mode network	+1	-61	+38
Lateral region of the sensorimotor network (left)	-55	-12	+29
Lateral region of the sensorimotor network (right)	+56	-10	+29
Superior region of the sensorimotor network	+0	-31	+67
Medial region of the visual network	+2	-79	+12
Occipital region of the visual network	+0	-93	-4
Lateral region of the visual network (left)	-37	-79	+10
Lateral region of the visual network (right)	+38	-72	+13
Anterior cingulate cortex of the salience network	+0	+22	+35
Insula of the salience network (left)	-44	+13	+1
Insula of the salience network (right)	+47	+14	+0
Salience network rostral prefrontal cortex (left)	-32	+45	+27
Salience network rostral prefrontal cortex (right)	+32	+46	+27
Supramarginal gyrus of the salience network (left)	-60	-39	+31
Supramarginal gyrus of the salience network (right)	+62	-35	+32
Frontal eye field of the dorsal attentional network (left)	-27	-9	+64
Frontal eye field of the dorsal attentional network (right)	+30	-6	+64
Intraparietal sulcus of the dorsal attentional network (left)	-39	-43	+52
Intraparietal sulcus of the dorsal attentional network (right)	+39	-42	+54
Lateral prefrontal cortex of the frontoparietal network (left)	-43	+33	+28
Lateral prefrontal cortex of the frontoparietal network (right)	+41	+38	+30
Posterior cingulate cortex of the frontoparietal network (left)	-46	-58	+49
Posterior cingulate cortex of the frontoparietal network (right)	+52	-52	+45
Inferior frontal gyrus of the linguistic network (left)	-51	+26	+2
Inferior frontal gyrus of the linguistic network (right)	+54	+28	+1
Posterior superior temporal gyrus of the linguistic network (left)	-57	-47	+15
Posterior superior temporal gyrus of the linguistic network (right)	+59	-42	+13
Anterior region of the cerebellum network (x=0, y=-63, z=-30)	+0	-63	-30
Posterior region of the cerebellum network (x=+0, y=-79,	+0	-79	-32